LEVEL II

REPORT SD-TR-80-19

Single-Layer Refraction Correction Model

Prepared by D. W. WHITCOMBE
Guidance and Control Division
Engineering Group
The Aerospace Corporation
El Segundo, Calif. 90245

15 November 1979

Final Report

Prepared for

SPACE DIVISION
AIR FORCE SYSTEMS COMMAND
Los Angeles Air Force Station
P.O. Box 92960, Worldway Postal Center
Los Angeles, Calif. 90009

This final report was submitted by The Aerospace Corporation, El Segundo, CA 90245, under Contract F04701-79-C-0080 with the Space Division, Deputy for Launch Vehicles, P.O. Box 92960, Worldway Postal Center, Los Angeles, CA 90009. It was reviewed and approved for The Aerospace Corporation by J. R. Allder, Engineering Group, and J. F. Wambolt, Programs Group. Col. R. C. Snavely, Space Division/YVXM, was the project engineer.

This report has been reviewed by the Public Affairs Office (PAS) and is releasable to the National Technical Information Service (NTIS). At NTIS, it will be available to the general public, including foreign nationals.

This technical report has been reviewed and is approved for publication. Publication of this report does not constitute Air Force approval of the report's findings or conclusions. It is published only for the exchange and stimulation of ideas.

R. C. Snavely

R. C. Snavely, Col., USAF
Medium Launch Vehicle Division
Deputy for Launch Vehicles

FOR THE COMMANDER

Joseph D. Mirth

Joseph D. Mirth
Colonel, USAF
Deputy for Space Launch Systems

UNCLASSIFIED

SECURITY CLASSIFICATION OF THIS PAGE (When Data Entered)

REPORT DOCUMENTATION PAGE	READ INSTRUCTIONS BEFORE COMPLETING FORM
1. REPORT NUMBER: 18 SD-80-19 19 TR-80-19 / 2. GOVT ACCESSION NO.: AD-A084 637	3. RECIPIENT'S CATALOG NUMBER
4. TITLE (and Subtitle): 6 SINGLE-LAYER REFRACTION CORRECTION MODEL,	5. TYPE OF REPORT & PERIOD COVERED: 9 Final rept,
	6. PERFORMING ORG. REPORT NUMBER: 14 TR-0080(5450-01)-1
7. AUTHOR(s): 10 D. W. Whitcombe	8. CONTRACT OR GRANT NUMBER(s): 15 F04701-79-C-0080
9. PERFORMING ORGANIZATION NAME AND ADDRESS: The Aerospace Corporation, El Segundo, Calif. 90245	10. PROGRAM ELEMENT, PROJECT, TASK AREA & WORK UNIT NUMBERS: 12 49
11. CONTROLLING OFFICE NAME AND ADDRESS: Space Division, Air Force Systems Command, Los Angeles, Calif. 90009	12. REPORT DATE: 11 15 Nov [redacted] 79
	13. NUMBER OF PAGES: 57
14. MONITORING AGENCY NAME & ADDRESS (if different from Controlling Office)	15. SECURITY CLASS. (of this report): Unclassified
	15a. DECLASSIFICATION/DOWNGRADING SCHEDULE

16. DISTRIBUTION STATEMENT (of this Report)

Approved for public release; distribution unlimited.

17. DISTRIBUTION STATEMENT (of the abstract entered in Block 20, if different from Report)

18. SUPPLEMENTARY NOTES

19. KEY WORDS (Continue on reverse side if necessary and identify by block number)

Refraction	Troposphere
Ray-Bending	Ray Tracing
Radar	
Optical	

20. ABSTRACT (Continue on reverse side if necessary and identify by block number)

A single-layer tropospheric refraction model is developed for use in real time with C-band and X-band radars when tracking satellites or powered rocket vehicles above the troposphere ($\approx$25 km). Corrections for range and elevation angle are provided that are usable for all elevation angles above the horizon. The correction uses only the surface refractivity so that some unavoidable error due to moisture variations is introduced below

DD FORM 1473 (FACSIMILE)

UNCLASSIFIED 407710

SECURITY CLASSIFICATION OF THIS PAGE (When Data Entered)

19. KEY WORDS (Continued)

20. ABSTRACT (Continued)

elevation angles of ≈2 deg. In general, the correction is accurate to ΔR ≈ 2 ft and ΔE ≈ 0.001 deg when the radar elevation angle is greater than 2 deg, hence velocity errors resulting from elevation angle error buildup are minimized.

The method presented in this report is more accurate than simple models in use and is more rapid and economical than ray tracing.

CONTENTS

FIGURES

TABLES

SECTION I

INTRODUCTION

C-band and X-band radars are commonly used to track satellite and powered-rocket vehicles. The resulting measurements--range, azimuth angle, and elevation angle--are processed in a navigation computer to obtain the ephemeris or trajectory of the target vehicle. In general, the radar is located on the ground and the target vehicle is above the earth troposphere ($\approx$25 km). Hence the radar measurements are altered from their geometric values by tropospheric refraction.* The actual (geometric) value for the range may be 7 to 600 ft less than the measured range. Although there is negligible change in the azimuth angle, the actual (geometric) value of the elevation angle may be 30 mrad less than the measured value. Thus, it is necessary to correct the radar measurements for tropospheric refraction before they are processed in the navigation computer.

Simple formulae that were used for the Atlas and the Gemini launch vehicle radar corrections are given in Refs. 1 and 2. These equations are included in Appendix B. The Atlas real time correction [1] is in error by 0.01 deg when $E_o = 6$ deg and by 0.05 deg when $E_o = 3$ deg. The somewhat more sophisticated Gemini correction [2] reduces the error to 0.005 deg when $E_o = 6$ deg and 0.02 deg when $E_o = 3$ deg. In both cases, the error increases rapidly below $E_o = 3$ deg. In addition, the range refraction correction error is often $\approx$100 ft at these low elevation angles. Clearly, errors of this magnitude can lead to significant navigation and ephemeris errors. One of the most serious errors is the increasing velocity error that arises from the increasing refraction errors that result when simple formulae are used.

*The ionospheric refraction correction is essentially negligible at C-band and X-band radar frequencies.

This error buildup can provide velocity magnitude errors of several fps and pitch velocity errors up to 50 fps. Hence, it is desired that the refraction correction minimize this error buildup.

A simple refraction correction using a twelfth order polynomial in E_o is derived in Ref. 3. Even in this case, the accuracy below $E_o = 5$ deg deteriorates rapidly for lack of higher order terms.

More accurate refraction correction and analysis is often accomplished using a ray tracing program. These programs divide the troposphere between the radar and the target vehicle into many ($\approx$1000) layers, each having constant refractivity so that Snell's law of refraction may be used with each individual layer. They require many mathematical operations for each correction and therefore may not be usable for real time applications. Even with ray tracing programs, it is necessary to limit the bending in each layer to less than 1 mrad in order to preserve the accuracy of the technique.

An excellent procedure for correcting radar measurements for radar refraction is given in Ref. 4. This method curve fits the actual index of refraction profile using locally measured data (Rawinsonde) and integrates over this profile to obtain ΔE_o and ΔR. Unfortunately, the number of computations involved limits the technique to use in postflight reconstruction activities.

Simple refraction correction algorithms suitable for use in Real Time Applications are developed in this report. These require only the specification of the surface refractivity N_s* at the radar location. Reference 5 provides a detailed discussion of the rationale for using N_s in this manner. This simplification leads to some unavoidable error at low elevation angles (below 2 deg) because of the variation in surface moisture. The surface

*$N_s = W_s + D_s$ can be measured using local atmospheric pressure, wet bulb and dry bulb temperatures as shown in Appendix A.

refractivity N_s is the sum of wet and dry terms (D_s and W_s), and these have differing profiles with altitude. This error could amount to $\epsilon = (\Delta E_o) \approx 0.05$ deg, which is considered acceptable since most radars do not function well at these low elevation angles ($\approx$2 deg or less) because of ground multipath reflections. A correction could be devised that used W_s and D_s but at the expense of model complexity. For this reason this procedure is not followed herein.

The true range refraction correction is dependent upon the radar slant range, because the geometric distance traveled for the actual radar ray exceeds the geometric slant range to the target vehicle. This excess distance increases somewhat as the slant range increases. However, the variation is less than 2 ft whenever the elevation angle is greater than 2 deg. Hence it will be assumed in this analysis that the range refraction correction is independent of the radar slant range.

The improved refraction correction developed in this report assumes the entire troposphere is contained in a single layer with constant N_s. The height of the layer will vary to agree with empirical data discussed in Section II. The model development is discussed in the following sections:

II. Data Discussion
III. Single Layer Bending Model
IV. Slant Range Correction
V. Elevation Angle Correction
VI. Summary
VII. Validation

SECTION II

DATA DISCUSSION

The data for developing the improved refraction correction uses the Central Radio Propagation Laboratory (CRPL) exponential atmosphere model given in Ref. 6. Data are included for the following values of refractivity N_s, measured elevation angle E_o in mrad, and height H in km of the target vehicle:

$$N_s = 200,\ 252.9,\ 289,\ 313,\ 344.5,\ 377.2,\ 404.8,\ 450$$

$$E_o = 0,\ 1,\ 2,\ 4,\ 8,\ 15,\ 30,\ 65,\ 100,\ 200,\ 400,\ 900 \text{ mrad}$$

$$H = 10,\ 20,\ 30,\ 50,\ 70,\ 90,\ 110,\ 225,\ 350,\ 475 \text{ km}$$

Note from Ref. 6 that the total ray bending τ becomes constant and the radar slant range correction ΔR tends to become constant at heights above $\approx$25 km. The refraction correction developed herein will only apply when the target vehicle is above this altitude.

The CRPL data is included in Tables B-1 and B-2, giving the values of τ and ΔR for $200 \le N_s \le 450$ and $0 \le E_o \le 900$ mrad. Table B-2 includes the values for ΔR when the target vehicle is at three different altitudes. The top, middle, and bottom entries are for target altitudes of 50, 475, and 225 km, respectively. Note that a computation of ΔR when E_o = 90 deg is also included in the last column of Table B-2.

Empirical formulae will be developed in this report to essentially curve fit the data in Tables B-1 and B-2. Note that when the bending τ is known, a simple procedure allows the computation of the radar elevation angle refraction correction ϵ. The physical geometry of the single-layer model is discussed in Section III.

SECTION III

SINGLE LAYER BENDING MODEL

The geometry of the single layer bending model is shown in Fig. 1. The single layer of refractivity N_s and height h is shown as a shaded area. The radar at Point A measures an elevation angle E_o. The ray is refracted through the total bending angle τ on departure from the layer at Point B. The ray continues to the target vehicle at Point C.

The equation for Snell's law in spherical coordinates gives the following equation:

$$\mu_s \, a \cos E_o = (a + h) \cos \theta_1 \qquad (1)$$

where

$\mu_s = 1 + N_s \times 10^{-6}$

a = radius from earth center to the radar

θ_1 = elevation angle of ray after departure from layer

The law of sines for triangle OAB is as follows:

$$\frac{a + h}{\cos E_o} = \frac{a}{\cos (\theta_1 + \tau)} = \frac{R_1}{\sin (\tau + \theta_1 - E_o)} \qquad (2)$$

where R_1 is the length of the line $\overline{AB}$.

The law of sines for triangle OBC is

$$\frac{a + h}{\cos \theta} = \frac{r}{\cos \theta_1} \cong \frac{R - R_1}{\sin (\theta - \theta_1)} \qquad (3)$$

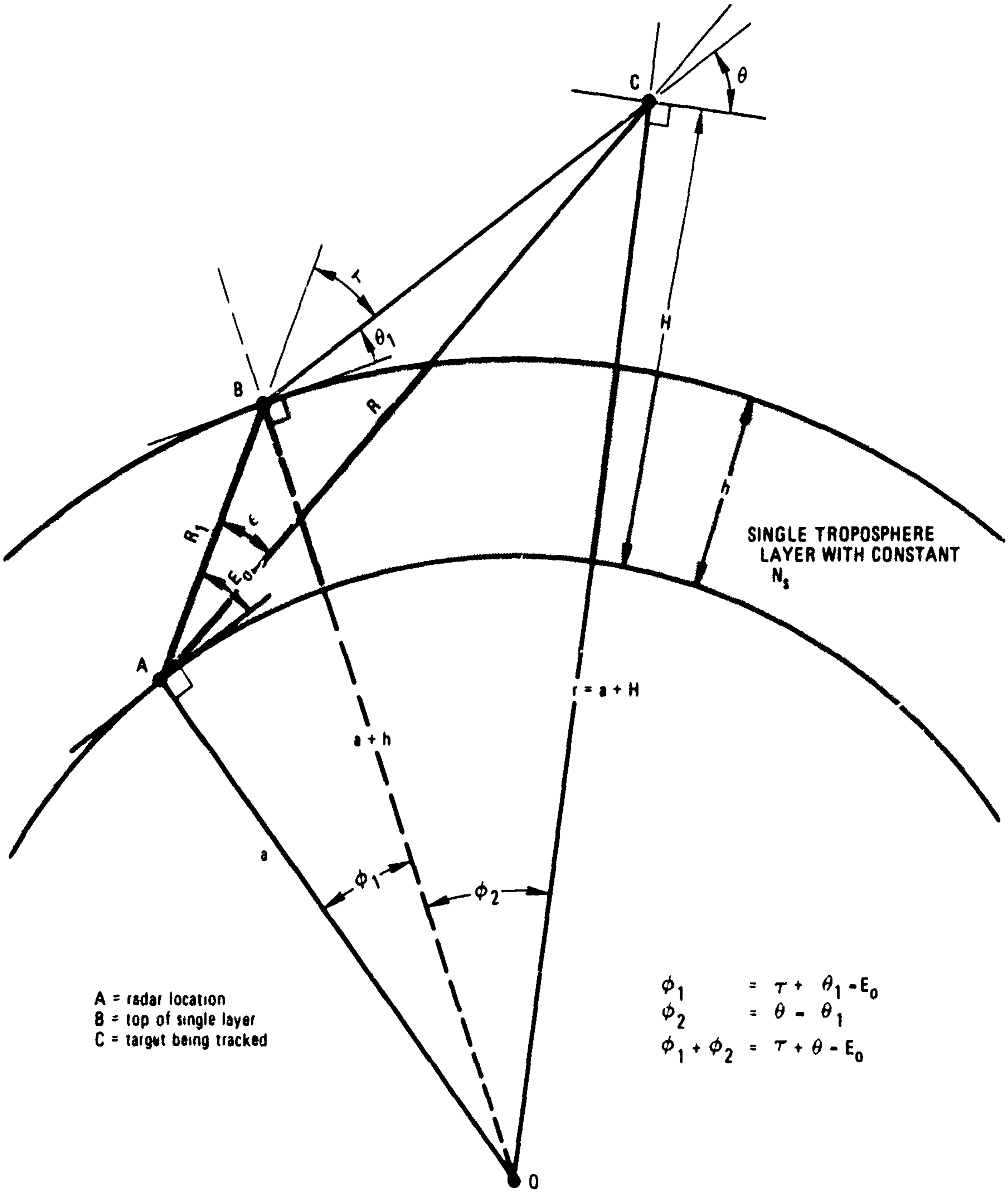

Fig. .1. Geometry of Single-Layer Refraction Model

where

r = distance from center of earth to target vehicle

R = geometric slant range from radar to target vehicle

θ = elevation angle of ray at target vehicle

The last term in Eq. (3) is not an equality because $\overline{AB}$ and $\overline{AC}$ are not colinear. However, the result is an excellent approximation.

The law of sines for triangle OAC is

$$\frac{a}{\cos(\theta + \tau - \epsilon)} = \frac{r}{\cos(E_o - \epsilon)} = \frac{R}{\sin(\tau + \theta - E_o)} \tag{4}$$

Equations (1) through (4) form the basis for the single layer model.

The first step in the analysis is to evaluate the thickness of the single layer such that the proper bending τ results. This is accomplished by solving Eqs. (1) and (2) for h after eliminating θ_1. The result is

$$h = \left[\frac{\cos E_o}{\cos(\theta_1 + \tau)} - 1\right] a \tag{5a}$$

where

$$\tan \theta_1 = \frac{\cos \tau - \frac{1}{\mu_s}}{\sin \tau} \tag{5b}$$

The results of the computation for h are included in Table B-3. Values for h in nmi are included for each case (E_o, N_s) for τ + 0.001 deg, τ, and τ - 0.001 deg. This technique permits an evaluation of the sensitivity of τ to the layer thickness. Note that when E_o <15 mrad the layer thickness must be accurate to about 20 to 50 ft. As E_o increases, the tolerance in the

layer thickness permits errors of several miles without causing the error in τ to exceed 0.001 deg.

The layer thicknesses along with the tolerances are now plotted in Fig. B-1. Note that the layer thickness is a linear function of N_s when the elevation angle is a constant. The best fit for h is given in nmi by

$$h = 1.2 + \frac{K}{1000}(620 - N_s) \tag{6}$$

where K is a function of E_o. The key variable in this computation is N_s. That is, this computation does not depend upon the height above sea level of the radar. Hence, regardless of radar height, a = 3444 nmi.

Equation (6) is then solved for K using the data in Table B-3. The results are given in Table B-4. Note that, as before, values are calculated for $\tau + 0.001$ deg, τ, and $\tau - 0.001$ deg. The resulting values for K are plotted, along with tolerances, in Fig. B-2. As before, when $E_o \leq 15$ mrad, the tolerances are small; as $E_o \to 90$ deg the tolerances become large. The best fit for K/1000 is of the form

$$\frac{K}{1000} = 0.0083 - 0.0072\, e^{-0.0221\, E_o}$$

where E_o is in mrad.

This completes the empirical curve-fit process for the evaluation of τ. A summary of the equations follows:

$$K = 8.3 - 7.2\, e^{-0.0221\, E_o}$$

$$h = 1.2 + \frac{K}{1000}(620 - N_s) \qquad \text{(cont.)}$$

$$\mu_s a \cos E_o = (a + h) \cos \theta_1 \tag{7}$$

$$(a + h) \cos (\theta_1 + \tau) = a \cos E_o$$

$$a = 3444$$

These equations were used to compute τ for each of the N_s, E_o data cases of Table B-1. The results are given in Table B-5. The maximum error is $\approx$0.05 deg when $E_o = 0$. Other errors are as large as 0.005 deg, but most errors do not exceed 0.001 deg for $E_o \geq 1$ deg and $252.9 \leq N_s < 377.2$.

SECTION IV

SLANT RANGE CORRECTION

The slant range correction ΔR is based on an observation by C. Brown, of the General Electric Company, Syracuse, N. Y. Brown noticed that when ΔR was large, it was nearly proportional to the ray bending τ; also that when $\tau = 0$, $\Delta R \cong 7$ ft. Hence, the expression

$$\frac{\Delta R - 7}{\tau}$$

was computed for the data listed in Tables B-1 and B-2.* The results are given in Table B-6 and plotted versus N_s in Fig. B-3. It was noted that slopes of $(\Delta R - 7)/\tau$ tended to be constants when E_o was constant. Since the slope was evaluated as 1/25, the following expression

$$b = \frac{\Delta R - 7}{\tau} + \frac{N_s}{25}$$

was evaluated (See Table B-7 for the results). Note that the values of b are closely grouped for constant elevation angles. Central values for the groups are listed as $\overline{b}$. Values for $37.2 - \overline{b}$ were then plotted in Fig. B-4, which shows an excellent straightline fit on log-log graph paper. Hence, b was evaluated as

$$b = 37.2 - 0.232\, E_o^{0.604}$$

*Values for ΔR in Table B-2, applicable to a target altitude of 475 km, are used.

These values also are listed as b-calc in Table B-7.

Hence the resulting expression for ΔR in feet becomes

$$\Delta R = 7 + \tau \left(37.2 - \frac{N_s}{25} - 0.232\, E_o^{0.604} \right) \tag{8}$$

where τ and E_o are in mrad.

Values for ΔR were computed using the Ref. 6 values of τ from Table B-1 and given in Table B-8. Results are also given in Table B-8 for ΔR when the equations of Fig. 2 are used. Note that all values are within 1 or 2 ft over the pertinent values of N_s and E_o. Also, the errors in the computed values appear to be random. That is, no significant time varying bias exists that grows as the radar elevation angle decreases. Thus, velocity errors resulting from this type of error buildup should be nil.

As discussed in Section I, the approximate range refraction correction given by Eq. (8) is independent of the radar slant range. As shown in Table B-2, the approximation is accurate to ±2 ft when $E_o \geq 2$ deg. The error can be as large as 10 to 20 ft when $E_o \approx 0$. Equation (8) can be modified to include the geometric range correction ΔR_g by modifying the curve fit procedure given in this section. Then the term $(\Delta R - 7)/\tau$ would be replaced by

$$\frac{\Delta R - 7 - k \Delta R_g}{\tau}$$

where, from Fig. 1

$$\begin{aligned}\Delta R_g &= R_1 + \overline{BC} - R \\ &= R_1 + \overline{BC} - \left[R_1 \cos \epsilon + \overline{BC} \cos (\tau - \epsilon)\right] \\ &= 2R_1 \sin^2 \frac{\epsilon}{2} + 2\overline{BC} \sin^2 \frac{\tau - \epsilon}{2} \\ &\cong 2R_1 \sin^2 \frac{\epsilon}{2} + 2(R - R_1) \sin^2 \frac{\tau - \epsilon}{2}\end{aligned}$$

and k is derived from the best curve fit. This compensation for ΔR_g is not implemented in Eq. (8) because the expression is not planned for use below $E_o = 2$ deg.

SECTION V

ELEVATION ANGLE CORRECTION

An expression for the radar elevation angle refraction correction ϵ will now be derived. It is assumed that the measured radar slant range R^* and E_o are known. The procedure for this calculation using Eqs. (1) through (4) is by no means unique. It is felt that the method included herein is one of the simpler methods.

Equations (7) and (8) are assumed to have been calculated so that h, θ, τ and ΔR are known. The procedure will use Eqs. (2), (3), and (4) to compute R_1, θ, and finally ϵ. The quantity R_1 can be computed from Eq. (2) as

$$R_1 = \frac{a + h}{\cos E_o} \sin (\tau + \theta_1 - E_o) \tag{9}$$

Equation (3), written as

$$\frac{a + h}{\cos \theta} = \frac{R - R_1}{\sin (\theta - \theta_1)}$$

can be solved for θ to obtain

$$\tan \theta = \tan \theta_1 + \frac{R - R_1}{(a + h) \cos \theta_1} \tag{10}$$

where

$$R = R^* - \Delta R \tag{11}$$

Equation (4) then gives

$$\cos (\theta + \tau - \epsilon) = \frac{a}{R} \sin (\tau + \theta - E_o) \tag{12}$$

which can be solved for ϵ.

A sensitivity analysis was performed to evaluate the need for Eq. (11). It was found that an error of 1 km in slant range R results in an error in ϵ of 0.002 mrad or less when the vehicle is above an altitude of 20 km or greater. Therefore, the radar measured slant range R^* can be used for R in Eqs. (10) and (12).

SECTION VI

SUMMARY

A block diagram of the single layer radar refraction correction equations is given in Fig. 2. The E_o and R^* are measured by the radar in radians and feet, respectively, while N_s is measured using the procedure described in Appendix A. The computational procedure shown in the block diagram results in the elevation angle refraction correction in radians and ΔR in feet.

For some areas it may be desirable to "fine-tune" the constants in the block diagram from their nominal values of

$$K_1 = 8.3 \qquad K_6 = 37.2$$
$$K_2 = 7.2 \qquad K_7 = -0.232$$
$$K_3 = 22.1 \qquad K_8 = 0.604$$
$$K_4 = 1.2 \qquad K_9 = 7$$
$$K_5 = 620 \qquad K_{10} = 25$$

in order to agree with ray-tracing programs using climatology data for a specific area. This is easily accomplished by varying the ten K constants and noting the effect on ε and ΔR. However, no such fine tuning has been found necessary for the VAFB area.

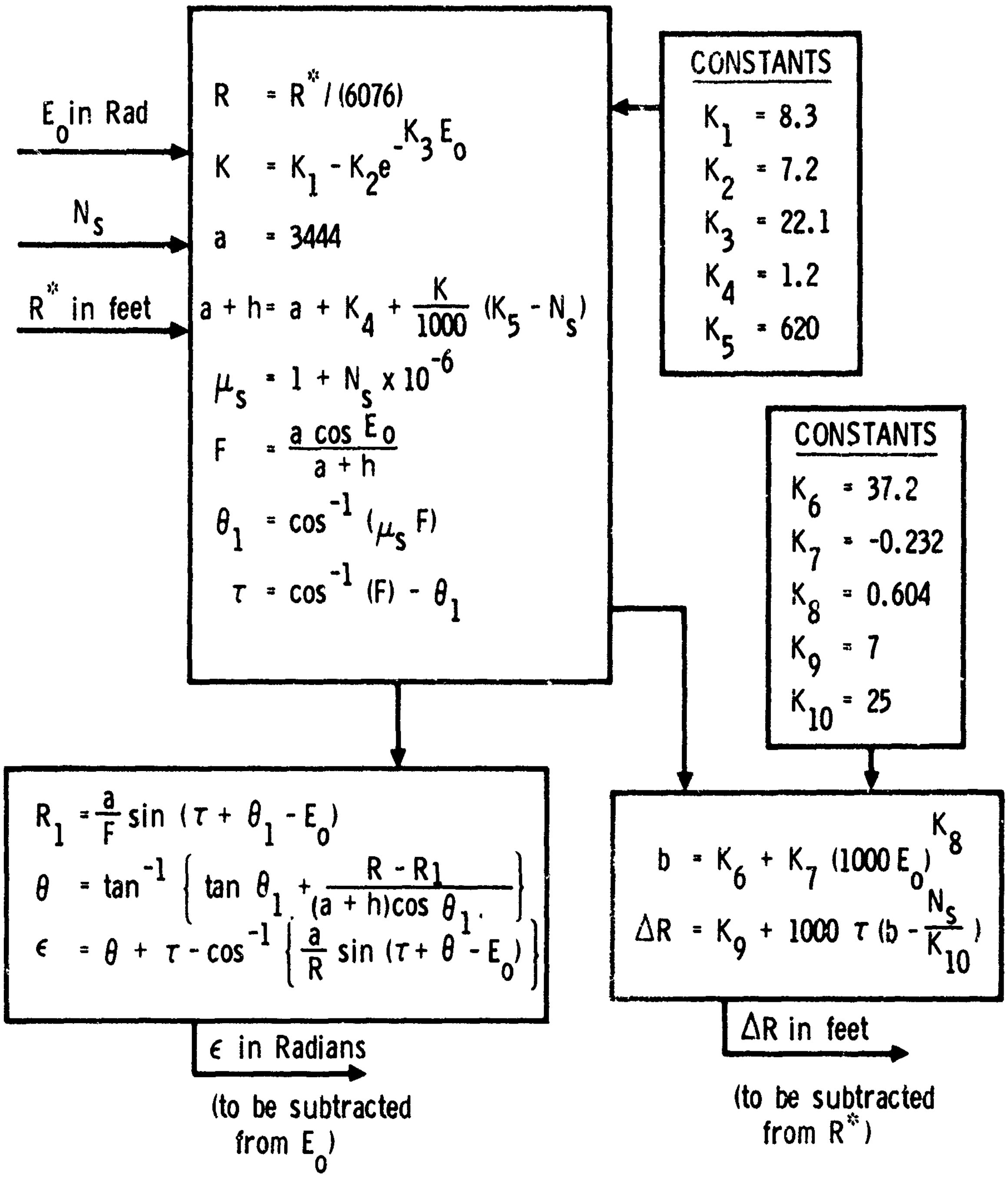

Fig. 2. Block Diagram of the Single-Layer Refraction Model Equations

SECTION VII

VALIDATION

The accuracy of the single-layer equations to compute the elevation angle refraction correction ϵ has been tested using the data in Ref. 6. The results are given in Table B-9. Note that in all except extreme cases the accuracy is good to $\approx$ 0.001 deg ($\cong$ 0.02 mrad). The ΔR computation test results for the same cases are given in Table B-8. These are accurate within $\approx$ 2 ft except for the extreme cases.

The equations of Fig. 2 with the nominal constant values have also been tested for three Atlas F flights launched from VAFB, and an Atlas SLV 3 flight launched from ETR. The results are given in Table B-10. The data on the correct values for ϵ and ΔR were supplied by C. Brown and obtained using his ray tracing program. Note that essentially all range corrections are within ± 5 ft and all elevation angle corrections are within ± 0.001 deg. These four flights span an N_s from 293 to 360. Hence, it is felt that the single layer refraction correction model with the equations given in Fig. 2 is sufficiently accurate for precision guidance and tracking purposes.

This testing also provides a validation of the computational procedure. All computations were performed using a Texas Instruments SR 52 which has 12 decimal ($\approx$ 40 bits plus sign) accuracy. Hence, double precision arithmetic may be required on the navigation computer. Floating point errors were only noted in computing τ when N_s = 450 and $0 \leq E_o < 15$ mrad. Special logic can be included to prevent floating point errors in this case.

The computational procedure will give excellent results ($\Delta\epsilon \cong$ 0.001 deg, $\Delta R \cong$ 2 ft) when the target vehicle is above an altitude of 25 km ($\cong$ 13.5 nmi) for $E_o \leq 100$ mrad. When $E_o \geq 900$ mrad, this altitude may be reduced by 50% to 12.5 km (6.75 nmi).

REFERENCES

1. J. L. Shores, Atlas-WTR Multipurpose Guidance Equations, Rev. A, GDC-BKM68-037, General Dynamics Convair, San Diego, Ca (July 1968).

2. D. G. Frostad and A. Linquitti, Equations and Program Specification for the Burroughs Mod III (A-1) Guidance Computer for the First Gemini Titan Launch Vehicle (GT-1), TOR-269(4126)-13, The Aerospace Corporation, El Segundo, Ca (10 January 1964).

3. T. A. Jagen, Analysis of WS-107A-2 Elevation Compensation Equations for Atmospheric Refraction Under Real Conditions, Tech Memo 64-4264-2, Bell Telephone Laboratories (1 April 1964).

4. H. M. Wachowski, A Model for Correcting Radar Tracking Data for the Effects of Tropospheric Refraction, TOR-0074(4461-02)-4, The Aerospace Corporation, El Segundo, Ca (2 July 1973).

5. B. R. Bean and E. J. Dutton, Radio Meteorology, National Bureau of Standards, Monograph 92 (1 March 1966).

6. B. R. Bean and G. D. Thayer, CRPL Exponential Reference Atmosphere, U.S. Dept. of Commerce, National Bureau of Standards, Monograph 4 (29 October 1959).

7. O. W. Eshbach, Handbook of Engineering Fundamentals, John Wiley & Sons, New York, N.Y. (1936).

8. F. A. Berry, E. Bolloy, and N. Beers, eds., Handbook of Meteorology, McGraw-Hill Book Co., Inc., New York (1945).

APPENDIX A

COMPUTATION OF N_s

The surface refractivity N_s may be computed using T_D, T_W, and P, where

T_D = dry bulb temperature, ^oF

T_W = wet bulb temperature, ^oF

P = barometric pressure, mbar
(1013.25 mbar = 760 mm Hg = 14.7 lb/in.^{2})

Then N_s is the sum of dry and wet terms:

$$N_s = D_s + W_s \tag{A-1}$$

where

$$D_s = 77.6 \frac{P}{T} \tag{A-2}$$

and

$$W_s = \left(\frac{3.75 \times 10^5}{T} - 6\right)\frac{e}{T} \tag{A-3}$$

with e = the actual water vapor partial pressure, mbar

T = the dry bulb temperature, ^oK

Then

$$T = \frac{5}{9}(T_D - 32) + 273.15$$

Eshbach (Ref. 7) shows that e may be evaluated as

$$e = e_s(x) - 0.000367\, P\, (T_D - T_W) \left(\frac{T_W + 1539}{1571}\right)$$

where $e_s(x)$ is the saturated water vapor pressure at the wet bulb temperature T_W in millibars.

Reference 8 shows that an excellent approximation to the saturated water vapor pressure in millibars is given by

$$e_s(x) = 6.11 \times 10^{7.5x/(237.3 + x)}$$

where

$$x = \frac{5}{9}(T_W - 32)$$

In some applications, T_W is not measured. The surface refractivity can be computed using Eqs. (A-1), (A-2), and (A-3) when relative humidity RH is given in place of T_W. In this case, the value for e required in Eq. (A-3) is computed as

$$e = \frac{RH}{100}\, e_s(y)$$

where

$$y = \frac{5}{9}(T_D - 32)$$

Note that $e_s(y)$ is the saturated water vapor pressure in millibars evaluated at the dry bulb temperature.

In other applications, the dew point temperature T_{DEW} in degrees Fahrenheit is measured. Then the partial pressure e required in Eq. (A-3) is given by

$$e = e_s(z)$$

where

$$z = \frac{5}{9}(T_{DEW} - 32)$$

APPENDIX B

SIMPLE REFRACTION CORRECTIONS

Atlas missile real-time correction (Ref. 1):

$$\Delta E = N_s \times 10^{-6} \cot E_o \left\{ 1 - \frac{1}{C_E S \sin E_o} \right\} \text{, in rad}$$

$$\Delta R = - \frac{N_s \times 10^{-6}}{C_E \sin E_o} \text{ in km}$$

$$C_E = \log \frac{N_s}{N_s + \Delta N}$$

$$\Delta N = -7.32\, e^{0.005577 N_s}$$

where

E_o = elevation angle measured from the local horizontal

S = slant range from radar to vehicle measured in kilometers

N_s = surface refractivity in n-units

$= (\mu_s - 1) \times 10^6$

μ_s = surface value (at radar) of the index of refraction

Gemini real-time correction (Ref. 2):

$$\Delta E = N_s \times 10^{-6} \cot E_o \left\{ 1 - \frac{1}{C_E S \sin E_o} \left[1 + \frac{S}{2a \sin E_o} \right] \right\} \text{, in radians}$$

ΔR = same as above

a = earth radius = 6373 km

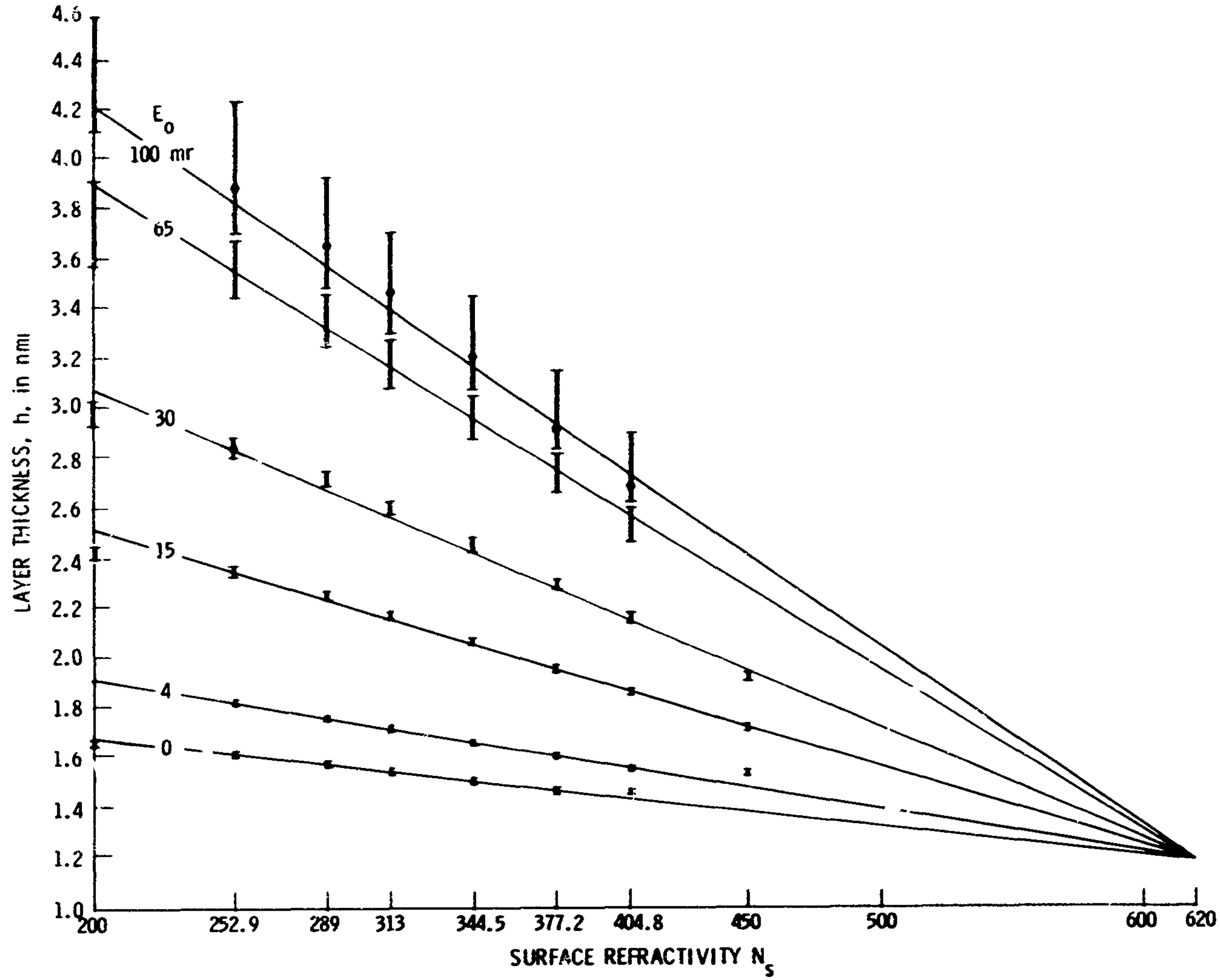

Fig. B-1. Plots of the Thickness h in nmi versus E_o and N_s of the Single Layer of Constant Refractivity N_s, as Tabulated in Table B-3

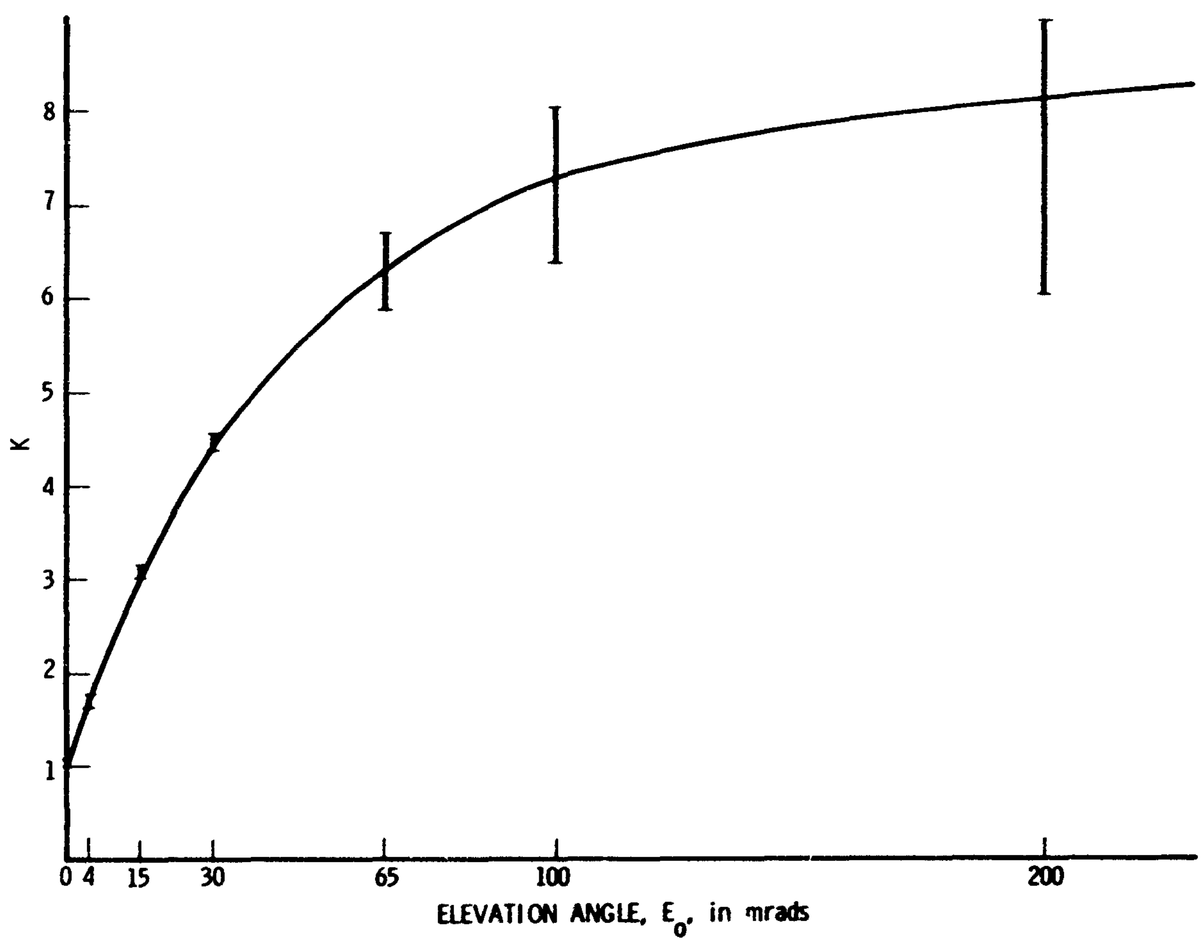

Fig. B-2. Plot of K versus Elevation Angle as Tabulated in Table B-4

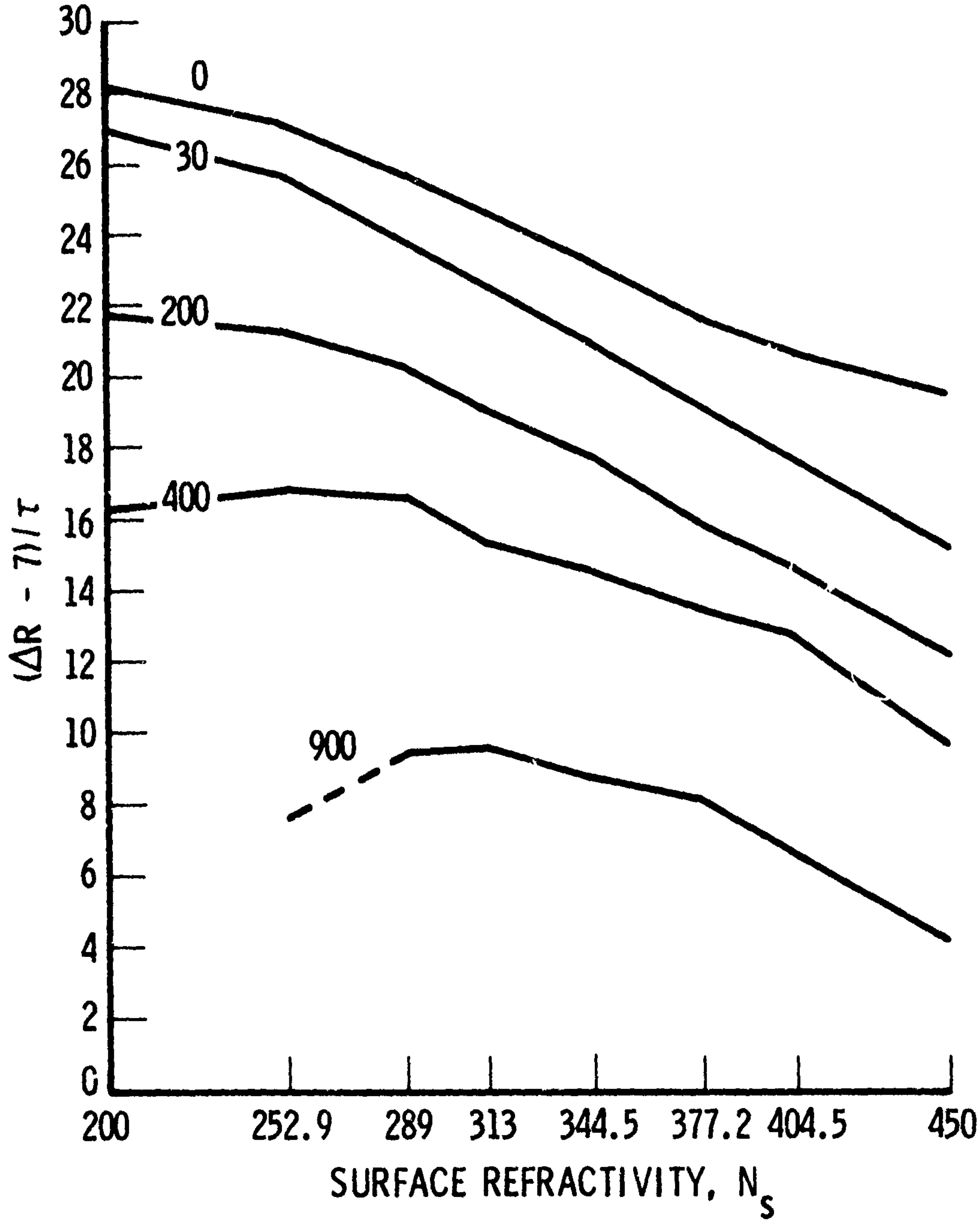

Fig. B-3. Plots of (ΔR - 7 ft)/τ versus E_o and N_s

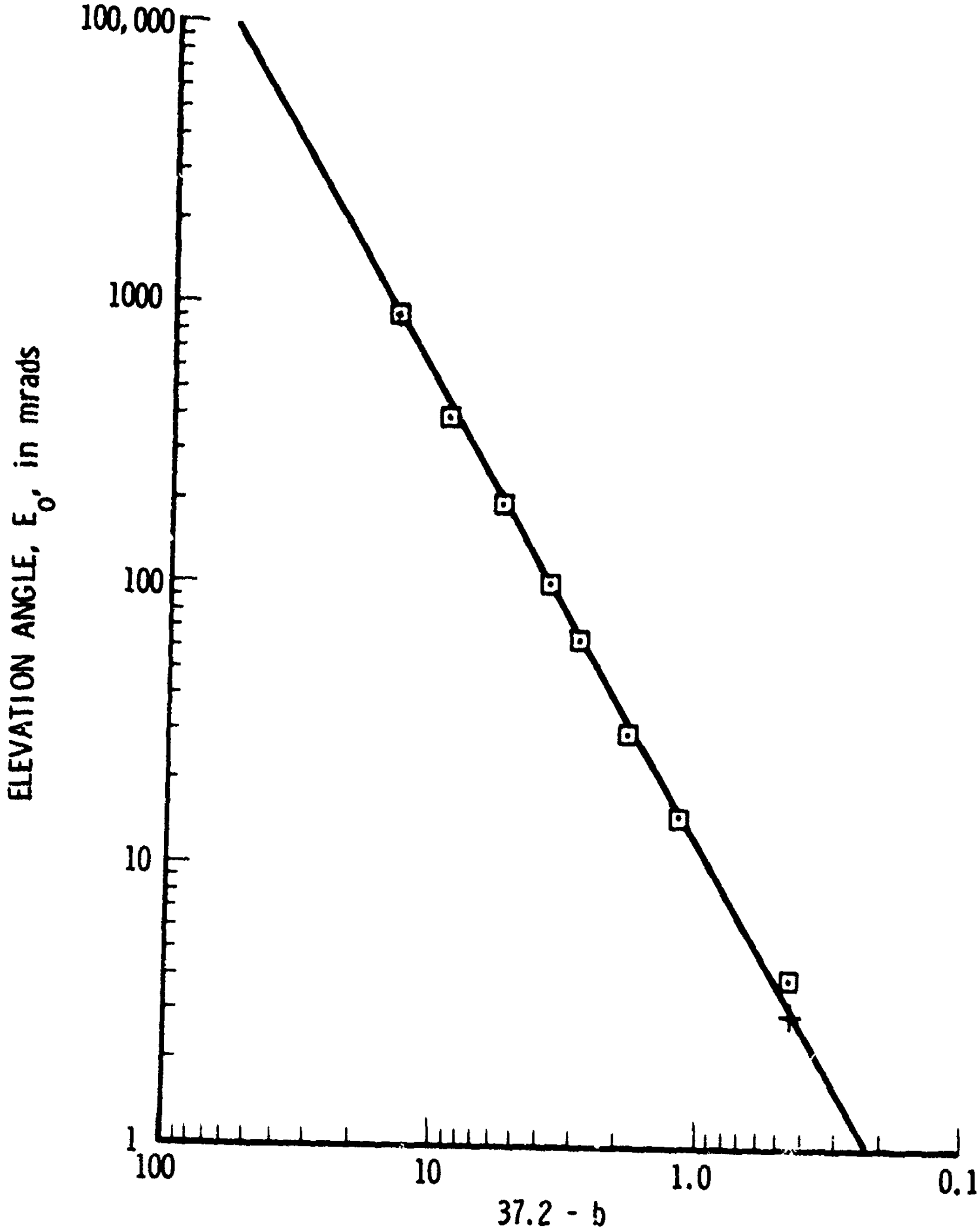

Fig. B-4. Plots of $37.2 - \bar{b}$ versus E_o

Table B-1. Total Ray Bending Data, τ in mrad, as Presented in Ref. 6 as a Function of N_s and E_o when the Target Vehicle is Above the Troposphere ($\approx$25 km).

N_s	Elevation Angle, E_o, in mrads								
	0	4	15	30	65	100	200	400	900
200	7.34217	6.68373	5.30065	4.06202	2.53741	1.80513	0.957793	0.45933	0.15542
252.9	9.83783	8.89787	6.96301	5.27446	3.25123	2.30005	1.21424	0.593733	0.200313
289	11.9413	10.7229	8.27128	6.18962	3.76356	2.64759	1.39074	0.678859	0.228916
313	13.5825	12.1225	9.23754	6.84394	4.11657	2.88342	1.50891	0.735598	0.247955
344.5	16.1315	14.2483	10.6450	7.76507	4.59538	3.19868	1.66497	0.810226	0.272968
377.2	19.4269	16.9091	12.3045	8.80242	5.11028	3.53202	1.82778	0.887767	0.298928
404.8	22.9207	19.6192	13.8833	9.74390	5.55795	3.81779	1.96594	0.953375	0.320875
450	31.516	25.73	17.0118	11.4653	Data Not Supplied in Ref. 6		2.19295	1.06069	0.356731

Table B-2. Total Range Refraction Error ΔR (ft) Based on Values Presented in Ref. 6 as a Function of N_s and E_o when the Target Vehicle Altitude is 50 km (top value), 475 km (center value) and 225 km (bottom value).*

N_s	Elevation Angle, E_o, in mrads									
	0	4	15	30	65	100	200	400	900	1570.8
200	211.5 213.9 213.9	191.7 193.8 193.8	151.3 152.2 152.2	115.8 116.1 116.1	72.5	51.5	27.9	14.76	7.15	5.54
252.9	269.3 273.6 273.2	242.0 245.7 245.7	187.6 189.3 189.3	141.4 142.4 142.0	87.2	61.7	32.8	17.06	8.56	6.57
289	307.4 314.2 313.2	273.9 278.1 277.2	208.7 210.9 210.9	154.6 155.1 155.1	93.5	66.3	35.1	18.37	9.18	6.983
313	333.6 341.8 340.5	295.0 300.4 299.8	221.0 223.4 223.4	162.0 163.0 163.0	96.8	67.9	35.8	18.37	9.41	7.136
344.5	370.3 381.8 379.8	322.8 330.6 329.3	235.4 239.4 238.8	169.2 170.6 170.2	99.4	68.6	36.7	18.89	9.43	7.2066
377.2	414.9 429.7 426.7	353.9 363.8 362.1	249.2 252.9 252.9	174.7 176.1 176.1	100.0	69.5	36.1	18.96	9.45	7.142
404.8	463.1 483.1 479.2	384.4 397.2 394.9	260.0 264.0 264.0	177.9 179.4 179.4	100.0	68.2	35.8	19.35	9.18	6.9954
450	591.7 630.4 621.6	454.3 474.6 471.0	277.1 283.4 282.1	179.3 180.7 180.7	Data not Supplied in Ref. 6		33.8	17.38	8.53	6.611

*When only one E_o value is given, the difference between these is negligible.

Table B-3. Height, h, of the Single Layer of Constant Refractivity N_s in nmi such that a Total Bending of τ + 0.001 deg, τ, and τ - 0.001 deg Results where τ is Presented in Table B-1.

N_s	Elevation Angle, E_o, in mrads								
	0	4	15	30	65	100	200	400	900
200	1.6382 1.644987 1.65184	1.8684 1.8775 1.88661	2.4 2.419 2.4376	2.9307 2.97138 3.0127	3.56584 3.73159 3.9013	3.6496 4.10517 4.57611	1.565 4.4827 7.5862	Results not Valid	
252.9	1.6104 1.6148 1.61927	1.8266 1.83266 1.83877	2.3263 2.3392 2.3522	2.82222 2.85193 2.88198	3.4202 3.54646 3.6751	3.5265 3.8799 4.2426	1.8972 4.20172 6.62128	-12.734 4.27985 23.0066	-184.6 4.13713 243.8
289	1.56421 1.56737 1.57055	1.7656 1.77003 1.77452	2.23069 2.24067 2.25072	2.69002 2.71402 2.73825	3.2394 3.34586 3.454	3.34118 3.6443 3.9543	1.9257 3.9348 6.0312	-10. 4.0409 20.3	-163. 4.0733 210.
313	1.5302 1.5326 1.5351	1.7187 1.7223 1.7259	2.15576 2.1641 2.1725	2.5861 2.60686 2.6279	3.0951 3.19056 3.2874	3.1862 3.46168 3.7429	1.8734 3.72174 5.644	-10. 3.8149 18.757	-152. 3.8443 193.
344.5	1.4887 1.49039 1.49207	1.6568 1.6594 1.662	2.0505 2.0570 2.0636	2.4376 2.45483 2.4722	2.88696 2.97015 3.0544	2.958 3.20273 3.4521	1.7456 3.4154 5.1456	-9.1 3.470935 16.97	-139. 3.40695 173
377.2	1.46004 1.46104 1.46204	1.6 1.60172 1.6035	1.9396 1.9446 1.9496	2.2774 2.29151 2.3058	2.6615 2.73402 2.8074	2.7102 2.92829 3.1501	1.5852 3.1008 4.6663	-8.4 3.14187 15.4	-128. 3.0757 157.
404.8	1.45969 1.46023 1.460776	1.567 1.5681 1.5692	1.8517 1.8557 1.8597	2.1447 2.1567 2.1688	2.4723 2.5373 2.603	2.50003 2.69906 2.9012	1.4261 2.83052 4.2779	-7.9 2.82334 14.203	-120. 2.60444 145.
450	Results not Valid	1.5586 1.5590 1.5593	1.7137 1.7163 1.7188	1.9223 1.9313 1.9404	Data not Supplied in Ref. 6		1.175 2.4276 3.7144	-7.2 2.46231 12.64	-108. 2.4739 130.

Table B-4. Computation of K/1000 where h = 1.2 + (K/1000) (620 - N_s) Using the Values of h Presented in Table B-3.*

N_s	Elevation Angle, E_o, in mrads: 0	4	15	30	65	100	200	400	900
200	0.001043 0.0010595 0.001076	0.001591 0.001613 0.001635	0.002857 0.002902 0.00295	0.004121 0.0042175 0.004316	0.005633 0.00599 0.006432	0.00583 0.006917 0.00804	0.000869 0.007816 0.01521	Results	not Valid
252.9	0.001118 0.00112994 0.0011421	0.00171 0.001723 0.00174	0.00307 0.003103 0.003139	0.004419 0.0044999 0.00458	0.00605 0.006392 0.006742	0.00634 0.0073 0.00829	0.0019 0.008177 0.01477	0.002 0.00839 0.05	0.002 0.008 0.6
289	0.001100 0.0011099 0.0011195	0.001709 0.001722 0.001736	0.003113 0.003144 0.003174	0.004502 0.004574 0.00465	0.00616 0.006483 0.00681	0.00647 0.0073846 0.00832	0.00219 0.008262 0.014596	0.002 0.00858 0.05	0.002 0.00868 0.63
313	0.001075 0.001083 0.001092	0.001689 0.0017013 0.001713	0.003113 0.0031404 0.003168	0.004515 0.004583 0.004651	0.006173 0.006484 0.0068	0.00647 0.007367 0.008283	0.002193 0.008214 0.01448	0.002 0.00852 0.005	0.002 0.00861 0.6
344.5	0.001048 0.001054 0.001060	0.001658 0.0016675 0.001677	0.003087 0.0031107 0.003135	0.004492 0.004555 0.004618	0.006123 0.006425 0.006731	0.006381 0.0072694 0.008175	0.00198 0.008041 0.01432	0.002 0.00824 0.005	0.002 0.00824 0.6
377.2	0.001071 0.001075 0.001079	0.016474 0.0016545 0.001662	0.003046 0.003067 0.003087	0.004437 0.004496 0.004554	0.00602 0.006318 0.00662	0.00622 0.0071182 0.008032	0.001586 0.0078287 0.014276	0.008	0.008
404.8	0.001207 0.00121 0.001211	0.0017054 0.0017105 0.001716	0.00303 0.003047 0.003066	0.00439 0.0044456 0.0044786	0.005912 0.006214 0.00652	0.006041 0.006966 0.007905	0.00105 0.007577 0.0143	0.00754	0.0065
450	Results	not Valid	0.00302 0.003037 0.003052	0.004249 0.004302 0.00436	Data not	Supplied in Ref. 6	0.00722 0.0148	0.0074	0.0075

*The three values in each box correspond to τ + 0.001 deg, τ, and τ - 0.001 deg where τ is the true value of total bending from Table B-1.

Table B-5. Computations of τ in mrad that Result Using the Single Layer Refraction Model when $h = 1.2 + (K/1000)(620 - N_s)$ and $K = 8.3 - 7.2e^{-0.0221E_o}$ as Required by Fig. 2.*

N_s	Elevation Angle, E_o, in mrads								
	0	4	15	30	65	100	200	400	900
200	7.293	6.597	5.199	3.99	2.510	1.794	0.957	0.469	0.158
252.9	9.888	8.915	6.947	5.253	3.240	2.296	1.214	0.594	0.2003
289	11.962	10.742	8.280	6.185	3.757	2.645	1.391	0.679	0.2289
313	13.541	12.109	9.244	6.842	4.110	2.880	1.5089	0.7357	0.2480
344.5	15.982	14.160	10.628	7.754	4.585	3.193	1.6644	0.8102	0.27296
377.2	19.308	16.759	12.243	8.770	5.092	3.523	1.8266	0.8876	0.2989
404.8	23.908	19.624	13.7927	9.693	5.533	3.806	1.964	0.9531	0.3208
450	Data cannot be calculated		16.887	11.359	6.283	4.278	2.1903	1.0604	0.3567

*These results compare favorably with the Ref. 6 results given in Table B-1.

Table B-6. Computations of $(\Delta R - 7\ \text{ft})/\tau$ for Values of ΔR in Table B-2 and Values of τ Presented in Table B-1.

N_s	Elevation Angle, E_o, in mrads								
	0	4	15	30	65	100	200	400	900
200	28.1796	27.948	27.393	26.859	25.538	24.652	21.821	16.176	0.951
252.[illegible]	27.099	26.827	26.18	25.671	24.668	23.782	21.248	16.944	7.788
289	25.726	25.282	24.652	23.934	22.904	22.398	20.205	16.749	9.523
313	24.649	24.203	23.426	22.794	21.814	21.121	19.087	15.457	9.7195
344.5	23.234	22.711	21.832	21.0687	20.107	19.258	17.838	14.6749	8.902
377.2	21.758	21.101	[illegible] 985	19.211	18.199	17.695	15.921	13.472	8.[illegible]96
404.8	20.772	19.889	18.511	17.693	16.733	16.030	14.649	12.954	6.7939
450	19.780	18.173	16.248	15.150	Data not Supplied in Ref. 6		12.221	9.786	4.289

Table B-7. Computation of $b = (\Delta R - 7)/\tau - N_s/25$.*

N_s	Elevation Angle, E_o, in mrads 0	4	15	30	65	100	200	400	900
200	36.179	35.948	35.393	34.859	33.538	32.652	29.821	24.176	18 [illegible]
252.9	37.215	36.943	36.29	35.726	34.784	33.898	31.364	27.06	17.90
289	37.286	36.842	36.185	35.494	34.464	33.958	31.765	28.309	21.083
313	37.169	36.723	35.946	35.314	34.334	33.641	31.607	27.977	22.2395
344.5	37.014	36.491	35.612	34.85	33.887	33.038	31.618	28.4549	22.68
377.2	36.846	36.189	35.073	34.3	33.287	32.783	31.009	28.[illegible]	23.284
404.8	36.964	36.081	34.703	33.885	32.925	32.222	30.841	29.146	22.98
450	37.78	36.173	34.248	33.15	Data not Supplied in Ref. 6		30.221	27.8	22.3
$\overline{b}$	37.2	36.75	36.	35.3	34.35	33.5	31.5	28.2	23.
b-calc	37.2	36.664	36.01	35.39	34.313	33.46	31.51	28.55	23.08

*The results show that b is approximately constant ($= \overline{b}$) when E_o is constant. Note results for $b_{calc} = 37.2 - 0.232 E_o^{0.604}$ are also given.

Table B-8. Calculated Results for ΔR in ft.*

N_s	Elevation Angle, E_o, in mrads: 0	4	15	30	65	100	200	400	900	1570.8
200	**221.4** 220.0	**198.6** 196.1	**155.5** 152.6	**118.26** 116.23	**73.77** 73.04	**52.95** 52.68	**29.51** 29.49	**16.44** 16.64	**9.344** 9.388	**7** 7
252.9	**273.4** 274.8	**243.2** 243.7	**187.3** 186.9	**140.31** 139.75	**85.67** 85.40	**60.68** 60.58	**32.97** 32.97	**17.94** 17.94	**9.597** 9.597	**7** 7
289	**313.2** 313.7	**276.2** 276.7	**209.2** 209.4	**154.50** 154.40	**92.63** 92.48	**67.24** 67.91	**34.74** 34.74	**18.53** 18.53	**9.637** 9.637	**7** 7
313	**342.2** 341.2	**299.7** 299.4	**224.0** 224.1	**163.52** 163.47	**96.71** 96.57	**67.36** 67.30	**35.65** 35.65	**18.79** 18.79	**9.618** 9.618	**7** 7
344.5	**384.8** 381.3	**333.1** 331.0	**243.6** 243.2	**174.80** 174.56	**101.36** 101.14	**69.93** 69.83	**36.52** 36.51	**18.97** 18.96	**9.538** 9.538	**7** 7
377.2	**436.6** 433.9	**371.8** 368.6	**264.4** 263.1	**185.71** 185.06	**105.24** 104.90	**71.87** 71.71	**37.01** 36.99	**18.95** 18.95	**9.389** 9.389	**7** 7
404.8	**488.5** 509.3	**408.6** 408.7	**282.1** 280.3	**194.05** 193.08	**107.71** 107.27	**72.91** 72.70	**37.11** 37.08	**18.78** 18.77	**9.210** 9.210	**7** 7
450	**612.1** Results not valid	**487.2**	**313.4** 311.1	**206.4** 204.5	**Data not Supplied in Ref. 5**		**36.62** 36.59	**18.19** 18.18	**8.812** 8.812	**7** .

*The top results in each box use the value for τ from Ref. 6 (Table B-1) and compute $\Delta R = 7 + \tau\,[37.2 - (N_s/25) - 0.232E_o^{0.604}]$. The bottom numbers compute ΔR using the algorithms of Fig. 2.

Table B-9. Computations of the Radar Elevation Angle Refraction Correction Compared with the Results from Ref. 6.*

N_s	E_o (rads)	R (km)	ϵ in mrads Actual Value from Ref. 6	ϵ calc in mrads using Single-Layer Model
200	0	836.6546 2184.4487	5.6129 6.6797	5.5295 6.6256
	0.030	792.6962 1980.81[illegible]	3.3577 3.7841	3.271 3.7024
	0.100	509.2089 1605.3422	1.5496 1.724	1.5249 1.7091
	0.200	316.1304 1544.9417	0.8332 0.9322	0.8275 0.9302
	0.400	125.8272 796.5385	0.3876 0.4562	0.3864 0.4560
	0.900	89.0684 593.7551	0.1387 0.1554	0.1387 0.1554
252.9	0	849.7316 2199.0916	7.5776 8.9643	7.5567 9.0017
	0.030	652.3268 1555.6414	4.2144 4.8298	4.1705 4.8021
	0.065	630.4977 1782.7841	2.7812 3.085	2.7595 3.0707
	0.100	510.4426 1607.3952	1.9919 2.2021	1.9812 2.1961
	0.200	316.4145 1224.8613	1.0656 1.1758	1.0654 1.1757
	0.400	174.8040 796.6942	0.5238 0.5784	0.5254 0.5787
	0.900	63.6831 593.7700	0.1678 0.1968	0.1687 0.1969

*Results are included for N_s = 200, 252.9, 289, 313, 344.5, 377.2, 404.8, and 450, and for several elevation angles in rad and radar ranges in km.

Table B-9. (Continued)

N_s	E_o (rads)	R (km)	ϵ in mrads Actual Value from Ref. 6	ϵ calc in mrads using Single-Layer Model
289	0.004	828.3	8.3872	8.3282
		977.8	8.7443	8.7043
		1107.0	8.9750	8.9478
		1744.5	9.6138	9.6132
		2544.3	9.9624	9.9721
	0.030	482.75	4.5822	[illegible]
		802.32	5.2177	5.1962
		1042.94	5.4419	5.4265
		1992.26	5.7982	5.7904
	0.065	343.09	2.8251	2.7914
		632.28	3.2495	3.2339
		1361.11	3.5247	3.5153
		2145.32	3.612	3.6042
	0.100	391.174	2.2124	2.2023
		620.228	2.3729	2.3660
		1197.152	2.5053	2.5006
		1961.548	2.5607	2.5569
	0.200	316.616	1.2319	1.2324
		1225.331	1.3497	1.3499
	0.400	174.834	0.6045	0.6063
		1046.312	0.6664	0.6668
	0.900	114.413	0.2096	0.2102
		593.779	0.2252	0.2253
313	0.0005	685.493	9.709	9.4922
		1145.062	11.182	11.0721
		1877.577	12.043	11.9771
		2583.073	12.407	12.3565
	0.008	953.616	9.0063	8.9505
		1814.749	9.9108	8.8947
		2520.042	10.1912	10.1833

Table B-9. (Continued)

N_s	E_o (rads)	R (km)	ϵ in mrads Actual Value from Ref. 6	ϵ calc in mrads using Single-Layer Model
313 (cont'd)	0.030	659.256 932.443 1996.006 2360.687	5.5778 5.9486 6.4257 6.4903	5.5482 5.9311 6.4197 6.4853
	0.065	498.7089 861.3179 2147.2183	3.4342 3.7214 3.9580	3.4142 3.7082 3.9495
	0.100	391.7167 620.9501 1609.8978	2.4327 2.5993 2.7737	2.4212 2.5909 2.7689
	0.200	396.7511 1546.6412	1.3787 1.4755	1.3785 1.4755
	0.400	174.8556 796.8787	0.6595 0.7189	0.6609 0.7193
	0.900	89.0742 315.5020 593.7874	0.2269 0.2408 0.2441	0.2233 0.2410 0.2442
344.5	0	884.9912 1280.1638 2603.2036	12.713 13.768 14.969	12.414 13.547 14.805
	0.008	813.9202 1208.5371	10.184 11.012	10.0379 10.9164
	0.030	663.5291 1051.0956	6.405 6.906	6.3584 6.8787
	0.065	500.3103 863.3327	3.884 4.183	3.8558 4.1636
	0.100	392.4572 722.4238 1964.1783	2.735 2.946 3.106	2.7178 2.9354 3.0987

Table B-9. (Continued)

N_s	E_o (rads)	R (km)	ϵ in mrads Actual Value from Ref. 6	ϵ calc in mrads using Single-Layer Model
344.5 (cont'd)	0.200	396.980 864.340	1.5328 1.6042	1.5304 1.6029
	0.400	174.884 531.960	0.7333 0.7849	0.7336 0.7850
	0.900	89.076 284.272	0.2474 0.2649	0.2477 0.2650
377.2	0.001	893.548 1289.283	.4.928 16.097	14.5811 15.8537
	0.015	769.143 1162.933	10.081 10.834	9.9306 10.7302
	0.065	637.354 1367.641	4.5351 4.8422	4.4988 4.8172
	0.100	513.805 1200.807	3.1732 3.3784	3.1514 3.3647
	0.200	233.055 473.818	1.6032 1.7173	1.5953 1.7128
	0.400	174.914 532.040	0.8115 0.8627	0.8102 0.8622
	0.900	63.687 439.813	0.2635 0.2938	0.2632 0.2937
404.8	0.002	901.200 1820.798	17.0052 19.0993	16.9299 19.2491
	0.030	673.089 1061.648	8.2303 8.7842	8.1217 8.7052
	0.100	393.974 724.536	3.3495 3.5631	3.3160 3.5402

Table B-9. (Continued)

N_s	E_o (rads)	R (km)	ϵ in mrads Actual Value from Ref. 6	ϵ calc in mrads using Single-Layer Model
404.8 (cont'd)	0.200	317.3348 1227.1027	1.8030 1.9238	1.7942 1.9202
	0.400	125.9572 532.1092	0.8492 0.9287	0.8459 0.9277
	0.900	38.8611 114.4221	0.2643 0.3015	0.2626 0.3010
450	0.015	945.4043 1713.1364	14.723 15.748	14.4888 15.5812
	0.030	681.7705 1590.2460	9.861 10.777	9.6748 10.6495
	0.200	233.4272 474.4563	1.9823 2.0893	1.9646 2.0793
	0.400	77.4153 797.3426	0.9012 1.0451	0.8907 1.0439
	0.900	38.8620 593.8329	0.3033 0.3532	0.3001 0.3530

Table B-10a. Data for Atlas Launch 65F (N_s = 330.692)

Flight Time (sec)	RADAR DATA		RAY TRACING RESULTS OF C. BROWN		CALC. RESULTS USING SINGLE-LAYER MODEL (FIG. 2)	
	E_o (deg)	Measured Range (ft)	ΔE^o	ΔR (ft)	ΔE^o	ΔR (ft)
130.4	35	341764.8	0.0238	11.8	0.0240	13.03
153.5	30	529068.5	0.0298	13.7	0.0300	14.87
185.6	25	816959.0	0.0378	16.3	0.0379	17.48
224.8	20	1226078.4	0.0489	20.2	0.0490	21.43
268.3	15	1779735.7	0.0665	26.7	0.0665	28.04
286.1	13	2046671.5	0.0769	30.6	0.0769	32.10
295.0	12	2190204.9	0.0833	33.1	0.0833	34.63
303.8	11	2341910.1	0.0906	36.0	0.0906	37.61
312.7	10	2502728.6	0.0993	39.4	0.0993	41.15
321.4	9	2669919.2	0.1099	43.5	0.1098	45.44
330.2	8	2850398.0	0.1224	48.4	0.1224	50.73
339.7	7	3044583.5	0.1383	54.8	0.1382	57.40
350.0	6	3257634.1	0.1583	62.9	0.1583	66.02
361.6	5	3495513.7	0.1849	73.8	0.1847	77.56
373.4	4	3739671.2	0.2211	88.9	0.2207	93.65
387.0	3	4018838.3	0.2736	111.0	0.2727	117.38

Table B-10b. Data for Atlas Launch 64F (N_s = 320.246)

	MEASURED DATA		RAY TRACING C. BROWN	Calculated Results (deg) Using Single Layer Model (Fig. 2)
Flight Time (sec)	E_o (deg)	Radar Range (ft)	ΔE (deg)	
129.2	35	344970.2	0.0230	0.0232
152.6	30	538297.7	0.0289	0.0290
184.7	25	831286.7	0.0366	0.0367
223.3	20	1240437.6	0.0473	0.0474
265.7	15	1785766.3	0.0648	0.0643
283.2	13	2049782.8	0.0743	0.0743
292.0	12	2192301.3	0.0804	0.0805
300.7	11	2341014.0	0.0875	0.0876
309.3	10	2498432.0	0.0959	0.0960
317.9	9	2663749.7	0.1060	0.1060
326.7	8	2844123.9	0.1183	0.1182
336.3	7	3040171.8	0.1335	0.1334
346.7	6	3253002.7	0.1528	0.1527
358.0	5	3486529.7	0.1783	0.1780
370.0	4	3734569.0	0.2129	0.2126
376.7	3.2691	3871939.6	0.2470	0.2465

Table B-10c. Atlas Launch 50F $N_s = 292.873$

MEASURED DATA		RAY TRACING C. BROWN		Calculated Results using Single-Layer Model (FIG. 2)	
E_o (deg)	Range (ft)	ΔR (ft)	ΔE (deg)	ΔR (ft)	ΔE (deg)
5.29064	6691691	70.19	0.1579	69.95	0.1590
8.05368	5102130	48.13	0.1092	48.25	0.1096
11.99223	3482100	33.06	0.0745	33.47	0.0747

Table B-10d. Atlas SLV 3 Launch (ETR) $N_s = 360.805$

MEASURED DATA		RAY TRACING C. BROWN		CALCULATED RESULTS USING SINGLE LAYER MODEL (FIG. 2)	
E_o (deg)	Range (ft)	R (ft)	E (deg)	R (ft)	E (deg)
29.8948	290495	13.86	0.0306	14.89	0.0308
10.6004	1917089	37.48	0.1020	39.67	0.1019
5.1890	3184124	72.53	0.1982	77.49	0.1968